Shaping the Skin: The Interplay of Mesoscale Geometry and Corneocyte Swelling

Myfanwy E. Evans[1,*] and Roland Roth[2]
[1]Institut für Theoretische Physik, Universität Erlangen-Nürnberg, 91058 Erlangen, Germany
[2]Institut für Theoretische Physik, Universität Tübingen, 72076 Tübingen, Germany
(Received 19 September 2013; published 24 January 2014)

The *stratum corneum*, the outer layer of mammalian skin, provides a remarkable barrier to the external environment, yet it has highly variable permeability properties where it actively mediates between inside and out. On prolonged exposure to water, swelling of the corneocytes (skin cells composed of keratin intermediate filaments) is the key process by which the stratum corneum controls permeability and mechanics. As for many biological systems with intricate function, the mesoscale geometry is optimized to provide functionality from basic physical principles. Here we show that a key mechanism of corneocyte swelling is the interplay of mesoscale geometry and thermodynamics: given helical tubes with woven geometry equivalent to the keratin intermediate filament arrangement, the balance of solvation free energy and elasticity induces swelling of the system, importantly with complete reversibility. Our result remarkably replicates macroscopic experimental data of native through to fully hydrated corneocytes. This finding not only highlights the importance of patterns and morphology in nature but also gives valuable insight into the functionality of skin.

DOI: 10.1103/PhysRevLett.112.038102 PACS numbers: 87.16.Ka, 05.70.-a, 87.85.J-

The skin is a large and complex organ whose numerous layers perform distinct functions, from insulation and temperature regulation to the sensation of touch. The outer layer, the stratum corneum, provides a necessary and robust boundary between conditions with distinct water concentrations inside and outside of the body [1]. Despite being *dead*, i.e., without organelles and blood supply, this layer plays an active role in the control of transepidermal water loss through variation of cell porosity and water diffusion properties [2], as well as providing a mechanical protection against infections.

Corneocytes actively regulate various functions by extreme, reversible swelling on prolonged exposure to water [3–6]. The swelling of corneocytes is intriguing for two key reasons: first, the expansion of corneocytes is beyond what is permitted via elastic extension of the component filaments (transformation from 35% keratin packing fraction in native skin to 15% in hydrated skin [4,5,7] is beyond a 150% extension of the intermediate filament length), and second, the swelling process is completely reversible over many repetitions. Experimental imaging [8] suggests that the geometry of the keratin intermediate filaments (IFs), the structural components of the corneocytes, is the Σ^+ rod packing [9] (geometric details are given in Fig. 1 and elsewhere [10,11]). At the very least, it is ordered and cubic [9]. Assuming the Σ^+ geometric arrangement of the IFs, the anomalous expansion of the corneocytes is permitted by the "dilatant" property of the Σ^+ packing [7]. In dilatant materials, the cooperative unwinding of curvilinear filaments in a chiral arrangement lever off each other and cause an expansion of the material beyond an isotropic stretching, somewhat related to "Auxetic" materials with a negative Poisson's ratio [12]. The reversal back to the compact state for symmetric dilatant materials is well defined and unique.

The dilatant behavior of the structure is a consequence of a precisely ordered, chiral pattern for the keratin IFs, a behavior unlikely for disordered networklike structures, particularly not in a reversible fashion. It is likely this pattern is formed via membrane templating [7,9], as the Σ^+ arrangement is closely related to the Gyroid minimal surface [11], a phase readily observed in lipid self-assembly [13]. The macroscopic consequences of mesoscale patterning *in vivo* is intriguing, reminiscent of the Gyroid chitin geometry in butterfly wings, which dictates macroscopic photonic effects in the form of structural color [14–16]. By exploring further these mesoscale geometric mechanisms within the skin cells, an approach proven to be instructive [17,18], we wish to provide a link between molecular scale and macroscopic science.

In this Letter, we consider the effect of thermodynamics on the system. We do this by examining the free energy balance for the helical Σ^+ rod packing over a range of configurations, from small to large unit cell size L, and from straight components through to a large helical radius R (Fig. 1). The keratin IFs are represented by helical tubes with radius $r = 3.7$ nm [19]. The helical tubes make two helical turns diagonally across the unit cell, and we require that the helical tubes never overlap. We alter the variables L and R until the tubes just touch.

The calculation of the solvation free energy F_{sol} of simple [20] and complex [21] solutes within the so-called morphometric approach [22–24] is highly efficient and accurate. F_{sol} (per unit cell) can be computed as a function

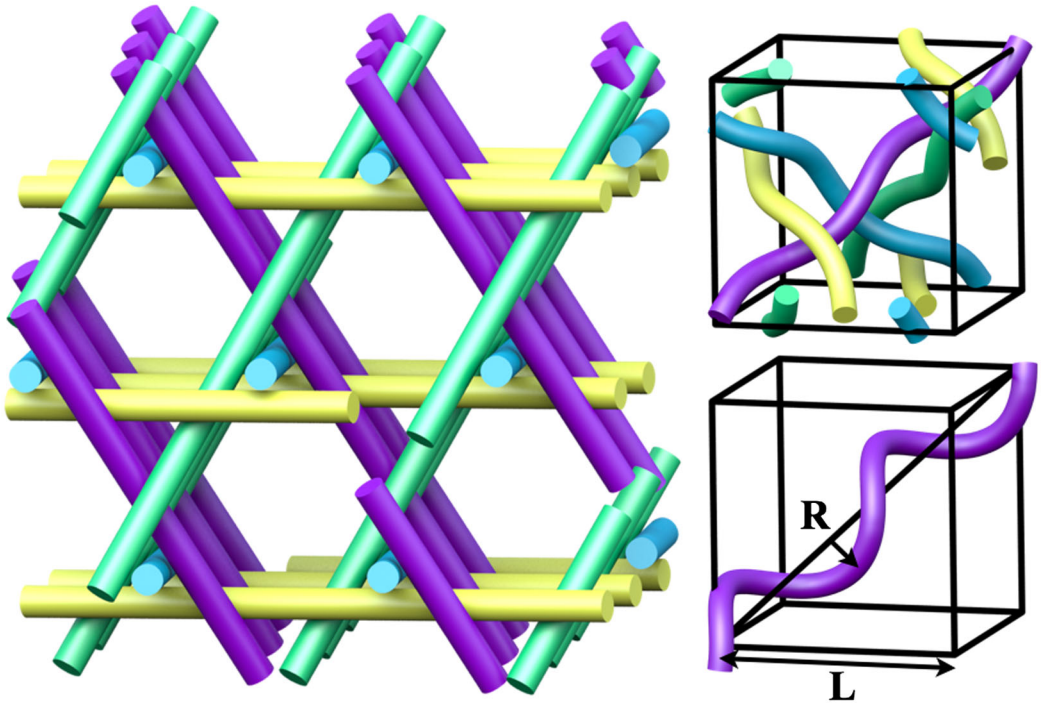

FIG. 1 (color online). (Left) The periodic Σ^+ rod packing composed of straight rods. (Right upper) One unit cell of the structure with slightly helical filaments. (Right lower) A single helix of the structure shown with the variable parameters: L is the unit cell edge length, R the radius of the helix. The tube radial thickness r is 3.7 nm, the radius of keratin IFs.

of only four purely geometric quantities, characterizing the shape of the solute, combined with thermodynamic prefactors that are independent of the specific geometry and are determined by the solvent-solvent and solvent-solute interactions:

$$F_{\mathrm{sol}} = pV + \gamma A + \kappa C + \bar{\kappa} X, \tag{1}$$

where the geometrical measures of the filaments per unit cell are the volume V, the surface area A, and the integrated (over the surface) mean (C) and Gaussian (X) curvatures. It is convenient to calculate these geometric measures for the solvent accessible surface, i.e., the surface that is accessible for the centers of solvent particles. Thus the radial thickness r increases by $R_s = 1.4$ Å, the radius of the solvent (s) which we set to the radius of water, and the volume excluded for centers of water can overlap, even if the underlying helical tubes do not. The corresponding thermodynamic coefficients in Eq. (1) re the solvent pressure p, the planar wall surface tension γ, and the bending rigidities κ and $\bar{\kappa}$ [20]. While the curvature terms in Eq. (1) are numerically smaller than the volume and especially the surface term, they still are of conceptual importance. All of the four terms in Eq. (1) depend on the definition of the dividing surface, but the sum of *all* four does not [24]. By focusing on the largest numerical contribution, the calculated solvation free energy would keep this definition dependency.

The geometric quantities required for the computation of F_{sol} can be calculated analytically, if the excluded volume does not overlap. Where the filaments are very close to each other, so that the excluded volume overlaps, the geometric quantities are computed numerically.

The void space of the geometry is filled with a waterlike solvent and gives rise to the grand potential per unit cell, with unit cell volume V_{cell}, of $\Omega = -pV_{\mathrm{cell}} + F_{\mathrm{sol}}$. The interaction between the helical tubes and the solvent is hydrophilic, as for keratin IFs. The thermodynamic coefficients p, γ, κ, and $\bar{\kappa}$, which are independent of the solute geometry, can be computed in a simple geometry via classical density functional theory (DFT) [25]. We consider the solvation free energy of a hydrophilic sphere with radius R for which the geometric measures are particularly simple. We calculate the solvation free energy for the sphere in two steps. First, we fix the position of the sphere and thereby make it into an external potential for the solvent. In this external field we minimize the DFT in order to obtain the inhomogeneous equilibrium density distribution $\rho(r)$ of the solvent (r is the radial distance from the center of the solute sphere). In a second step we calculate the total grand potential of the system Ω, where we make use of the fact that in equilibrium the density functional reduces to the grand potential $\Omega = \Omega[\rho(r)]$ [25]. From Ω we can extract the solvation free energy $F_{\mathrm{sol}}(R)$ of the sphere and $f_{\mathrm{surf}}(R)$, the excess surface free energy per area, via

$$f_{\mathrm{surf}}(R) = \frac{1}{A}[F_{\mathrm{sol}}(R) - pV] = \gamma + \kappa\frac{C}{A} + \bar{\kappa}\frac{X}{A}. \quad (2)$$

For a sphere (and our definition of X) we obtain $C/A = 1/R$ and $X/A = 1/(4\pi R^2)$, so that the thermodynamic coefficients γ, κ, and $\bar{\kappa}$ can be extracted from a quadratic fit in $1/R$ to numerical DFT calculations for various values of the radius R. The solvent used in our calculation is a square-well fluid that models the properties of water, at these length scales, at ambient conditions [26]. While at microscopic length scales the structure of water is strongly influenced by details of the water-water interaction, for the mesoscale IF geometry here, a much simpler square-well fluid can account for the solvation effects appropriately. In Fig. 2 we show the results of our DFT calculations (symbols) for solute sphere radii ranging from small to large together with the morphometric form with fitted thermodynamic coefficients (line). The thermodynamic coefficients from the fit, for our definition of the dividing surface, are $\beta\gamma R_s^2 = -0.099$, $\beta\kappa R_s = -0.835$, and $\beta\bar{\kappa} = -17.518$. In contrast to the liquid-gas surface tension, the thermodynamic coefficient γ and possibly its sign depend on the definition of the dividing surface—here we use the solvent accessible surface. Since γ cannot be measured directly, this is not a problem. The agreement between the morphometric form and the DFT data is excellent. To ensure consistency with the real system, we enforce the pressure p to be that of water at ambient conditions.

Rheological studies suggest that the elasticity of soft keratin IFs in corneocytes is most likely akin to the highly elastic protein IFs excreted as slime from Hagfish [27,28], which have nonlinear elastic behavior to extensions of around 150%, vastly different from the hard keratin in hair and nails. The initial stiffness of Hagfish IFs is 6.4 MPa, which increases on extension through strain hardening [27]. We approximate the (engineering) stress σ versus strain $\varepsilon = \Delta l/l_0 \equiv (l - l_0)/l_0$ curve for keratin IFs in corneocytes in the nonlinear elastic regime by $\sigma = \alpha\varepsilon + \beta\varepsilon^2$ where $\alpha = 6.4$ MPa and $\beta = 18$ MPa are obtained from

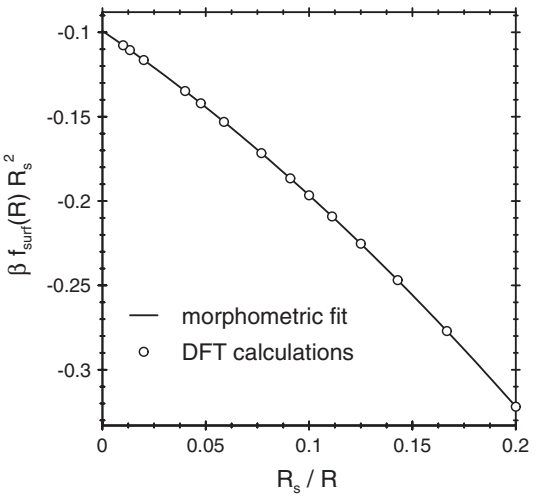

FIG. 2. The excess surface free energy per area $f_{\mathrm{surf}}(R)$ as function of the inverse solute sphere radius $1/R$. Symbols denote numerical values obtained from DFT calculations, while the full line represents the morphometric form with fitted thermodynamic coefficients γ, κ, and $\bar{\kappa}$. The agreement of the numerical DFT data with the morphometric form is excellent for all values of R.

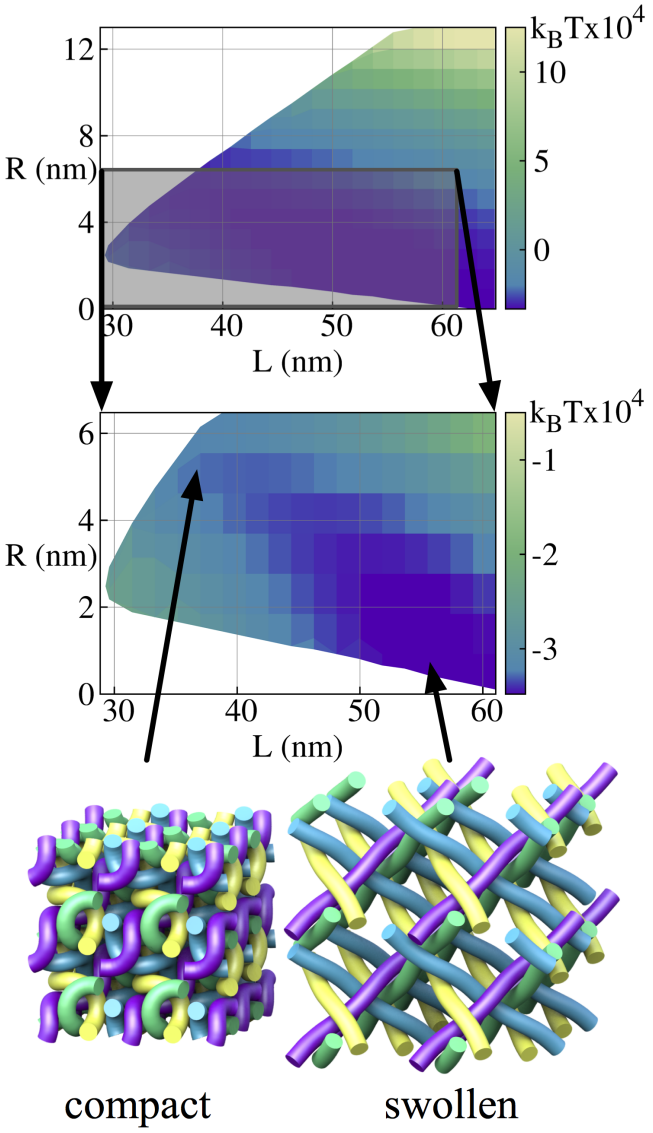

FIG. 3 (color online). Total free energy $\Omega + E$ (per unit cell) of the helical Σ^+ rod packing (Fig. 1), in units of $k_BT \times 10^4$ as a function of unit cell size L and helix radius R. The lower plot shows a smaller region of the upper plot. A valley of low total free energy configurations, whose extremes are indicated on the lower plot, traces a pathway for the swelling of corneocytes and subsequent drying. The packing fractions range from 11% to 38%, comparable to volume fractions (15%–35% [7]) that can be inferred from experimental hydration data [4,5].

a fit to the experimental stress-strain data for Hagfish slime given in Fig. 3(a) of [27]. We obtain an elastic energy E (per unit cell) by integration as

$$E(l) = \pi r^2 \left(\frac{\alpha}{2} \frac{\Delta l^2}{l_0} + \frac{\beta}{3} \frac{\Delta l^3}{l_0^2} \right). \quad (3)$$

We take the smallest possible unit cell geometry as having no elastic energy, thus $l_0 = 232$ nm.

We consider the combination of the grand potential Ω and the elastic energy E, where these are opposing: Ω minimizes with increasing volume and helical radius and E minimizes for decreasing volume and helical radius. The balance of these two opposing free energies is also typical of the swelling behavior of polymer gels [29,30]. Ω ranges from $-2.3 \times 10^4 k_B T$ when most compact to $-9 \times 10^4 k_B T$ for large unit cell length L and radius R. The range of E is from 0 when compact up to $30 \times 10^4 k_B T$ at largest L and R. When added together (Fig. 3), Ω dominates at small unit cell length and helix radius, and E dominates beyond a certain unit cell size and radius. The boundary between these two zones forms the minimal configurations of the total free energy, and passes somewhat linearly from the compact state at the point $L = 35$ nm and $R = 5.1$ nm to the global minimum of the system at $L = 55$ nm and $R = 1$ nm with decreasing total free energy. The total free energy at the global minimum is $-3.55 \times 10^4 k_B T$ and the total free energy is $-3.27 \times 10^4 k_B T$ at the compact state, marginally above the global minimum.

As a consequence of the minimal conformations of the total free energy landscape, we propose that the keratin IF geometry in corneocytes spans those configurations within the minimal valley, with the global minimum at the swollen state [31]. Thus, given water, the corneocyte will expand until it reaches the global minimum, where it is impeded from further expansion. The corneocytes then reverse back to the compact form once the water source in removed: only a small force is required (e.g., from evaporation) to transform back to this compact state. The packing fractions of 11% when swollen through to 38% when compact Fig. 3 are comparable values to volume fractions (15%–35% [7]) that can be inferred from experimental hydration data [4,5]. In addition, the change in length within this minimal pathway is well within the elastic regime of the keratin IFs, a property critical to the reversibility, and not possible with a disordered, cross-linked network structure.

Because of their hydrophilicity, the helical tubes remain without contacts for all favorable configurations, always having at least a thin layer of water lubricating between. This implies that IFs in corneocytes can easily slide across each other without cross-linking. Given that cross-linking is often dominant in the mechanics of random filament networks and biological materials [32], corneocytes might be softer than expected. The absence of cross-linking suggests causes for the complex mechanical profiles observed in experiments [33]. The delicate balance of competing energies in the system implies that overhydration or excessive drying of the system could cause filaments to come in contact and irreversibly cross-link, leading to macroscopic mechanical changes.

In other biomaterials, such as hair and nails, keratin IFs can also assemble into hard keratin, which has very different mechanical and hydration properties [28] to those of corneocytes. The highly cross-linked keratin matrix of mammalian hard keratins governs the mechanical properties of the biomaterial by preventing hydration of the keratin [34]. Thus the absence of cross-linking in corneocytes, which have a complex mechanical profile governed by extreme swelling, is unsurprising. It also suggests that corneocytes are held together by the complex entanglement of the filaments rather than connectivity between them. More practically, dermatitis is a common skin condition associated with physical changes in corneocytes, caused by excess hydration, excessive drying, external impact, or malfunctions in the initial cell growth process. Our results suggest that dermatitis could be related to irregular cross-linking of keratin IFs, which perturbs the hydration and mechanical profiles.

In this model, we treat the corneocyte as an infinite periodic material, rather than the reality of a finite cell surrounded by a lipid matrix. However, the relative size of the unit cell is very small in relation to the corneocyte, and thus boundary effects are limited. In addition to this, the system is considered through a succession of equilibrium states with a time scale on the order of hours for real corneocyte swelling, and thus the effect of water diffusion on the process is negligible.

The delicate energy balance and the easy expansion of the corneocytes is due to the fact that the grand canonical potential and the elastic energy of the system are comparable in magnitude. Altering either of these properties would drastically alter the balance of the system, changing the skin's ability to expand. For example, were the skin made of the hard keratin found in hair and nails, the elastic energy would dominate the system and prevent expansion, thus limiting the ability of the skin to actively adapt its barrier properties to the environment.

The water volume of corneocytes contains amino acids known as *natural moisturizing factors* (NMFs) [35,36], which prevent excessive evaporation of water. The upper end of the minimal free energy valley, which has a relatively low free energy compared with configurations adjacent to the valley, may provide a natural impedance to further drying of the corneocyte that is purely geometric, enhancing the effect of the NMFs. In addition, the porosity increase of the corneocytes with hydration supports the experimental evidence of increased diffusion for water through skin [2]. Within our model it should be possible to study the role of NMFs theoretically in more detail,

which in turn might result in insights and testable predictions on their behavior.

We have shown that macroscopic swelling of corneocytes is replicated by solvation and elasticity of helical tubes with woven geometry equivalent to the keratin IF arrangement. The balance of grand potential and elastic energy provides a range of conformations that span packing fractions of keratin IFs from native through to fully hydrated corneocytes. The global minimum of $\Omega + E$ is a swollen state: given water, the corneocyte will expand then reach a natural barrier to further swelling, yet easily transform to the compact form once again with only a small force from evaporation once the water source is removed. At all stages of the transformation from dry to hydrated, the IFs are contact free. This is a simple demonstration of how mesoscale geometry determines macroscale properties of biological materials: we have simplified the keratin IFs to helical tubes and replicated the swelling of corneocytes from geometry alone. This highlights the complex interplay of geometry and function in soft matter physics and biological systems.

M. E. thanks the Humboldt foundation and the DFG Forschergruppe "Geometry and Physics of Spatial Random Systems" for support. We thank Klaus Mecke, Bob Evans, and Erwin Frey for comments.

*myfanwy.e.evans@physik.uni-erlangen.de

[1] K. C. Madison, J. Invest. Dermatol. **121**, 231 (2003).
[2] I. H. Blank, J. Moloney, A. G. Emslie, I. Simon, and C. Apt, J. Invest. Dermatol. **82**, 188 (1984).
[3] L. Norlén, A. Emilson, and B. Forslind, Arch. Dermatol. Res. **289**, 506 (1997).
[4] P. Caspers, G. Lucassen, E. Carter, H. Bruining, and G. Puppels, J. Invest. Dermatol. **116**, 434 (2001).
[5] J. A. Bouwstra, A. de Graaff, G. S. Gooris, J. Nijsse, J. W. Wiechers, and A. C. van Aelst, J. Invest. Dermatol. **120**, 750 (2003).
[6] I. Willis, J. Invest. Dermatol. **60**, 166 (1973).
[7] M. E. Evans and S. T. Hyde, J. R. Soc. Interface **8**, 1274 (2011).
[8] I. Brody, J. Ultrastruct. Res. **2**, 482 (1959).
[9] L. Norlén and A. Al-Amoudi, J. Invest. Dermatol. **123**, 715 (2004).
[10] M. O'Keeffe, J. Plevert, Y. Teshima, Y. Watanabe, and T. Ogama, Acta Crystallogr. Sect. A **57**, 110 (2001).
[11] M. E. Evans, V. Robins, and S. Hyde, Acta Crystallogr. Sect. A **69**, 262 (2013).
[12] R. S. Lakes, Science **238**, 551 (1987).
[13] Z. Almsherqi, S. Kohlwein, and Y. Deng, J. Cell Biol. **173**, 839 (2006).
[14] K. Michielsen and D. G. Stavenga, J. R. Soc. Interface **5**, 85 (2008).
[15] V. Saranathan, C. O. Osuji, S. G. J Mochrie, H. Noh, S. Narayanan, A. Sandy, E. R. Dufresne, and R. O. Prum, Proc. Natl. Acad. Sci. U.S.A. **107**, 11676 (2010).
[16] G. E. Schröder-Turk, S. Wickham, H. Averdunk, F. Brink, J. D. F. Gerald, L. Poladian, M. C. J. Large, and S. T. Hyde, J. Struct. Biol. **174**, 290 (2011).
[17] S. T. Hyde, S. Andersson, K. Larsson, Z. Blum, T. Landh, S. Lidin, and B. W. Ninham, *The Language of Shape: The Role of Curvature in Condensed Matter: Physics, Chemistry and Biology* (Elsevier Science B.V., Amsterdam, 1997).
[18] Y. Snir and R. D. Kamien, Science **307**, 1067 (2005).
[19] R. D. Fraser, T. P. MacRae, D. A. Parry, and E. Suzuki, Proc. Natl. Acad. Sci. U.S.A. **83**, 1179 (1986).
[20] H. Hansen-Goos, R. Roth, K. Mecke, and S. Dietrich, Phys. Rev. Lett. **99**, 128101 (2007).
[21] R. Roth, Y. Harano, and M. Kinoshita, Phys. Rev. Lett. **97**, 078101 (2006).
[22] K. R. Mecke, J. Phys. Condens. Matter **8**, 9663 (1996).
[23] K. Mecke and C. H. Arns, J. Phys. Condens. Matter **17**, S503 (2005).
[24] P.-M. König, R. Roth, and K. R. Mecke, Phys. Rev. Lett. **93**, 160601 (2004).
[25] R. Evans, Adv. Phys. **28**, 143 (1979).
[26] R. Roth, D. Gillespie, W. Nonner, and R. E. Eisenberg, Biophys. J. **94**, 4282 (2008).
[27] L. Kreplak and D. Fudge, BioEssays **29**, 26 (2007).
[28] D. S. Fudge, T. Winegard, R. H. Ewoldt, D. Beriault, L. Szewciw, and G. H. McKinley, Integr. Comp. Biol. **49**, 32 (2009).
[29] M. Daoud, E. Bouchard, and G. Jannick, Macromolecules **19**, 1955 (1986).
[30] E. Geissler, F. Horkay, A. M. Hecht, and M. Zrinyi, J. Chem. Phys. **90**, 1924 (1989).
[31] See Supplemental Material at http://link.aps.org/supplemental/10.1103/PhysRevLett.112.038102 for an animation of the pathway from compact to swollen configurations of corneocytes.
[32] C. P. Broedersz, X. Mao, T. C. Lubensky, and F. C. MacKintosh, Nat. Phys. **7**, 983 (2011).
[33] J. D. Beard, R. H. Guy, and S. N. Gordeev, J. Invest. Dermatol. **133**, 1565 (2013).
[34] D. A. Greenberg and D. S. Fudge, Proc. R. Soc. B **280**, 20122158 (2012).
[35] R. L. Eckert, Physiol. Rev. **69**, 1316 (1989).
[36] A. V. Rawlings, I. R. Scott, C. R. Harding, and P. A. Bowser, J. Invest. Dermatol. **103**, 731 (1994).